Electronic Supplementary Material (ESI) for Inorganic Chemistry Frontiers.


# Supporting Information

## Tail of imidazole regulated assembly of two robust sandwich-type polyoxotungstates-based open frameworks with efficient visible-white-light-driven catalytic oxidation of sulfides

Xianqiang Huang*[a], Sen Liu[a], Zhen Zhou[c], Haizhen Zhang[a], Zongyin Gao[a], Guodong Shen[a], Huaiwei Wang,[a] Zhi Wang,*[b] Qingxia Yao[a], and Di Sun*[b]

# Table of contents

# 1. Experimental section.

## Materials and methods

Sodium tungstate dihydrate (Energy Chemical, 99%), sodium arsenate (Chengdu Aikeda Chemical Reagent Company, 99%), zinc chloride (Energy Chemical, 99%), 1-propyl imidazole, 1-isopropyl imidazole (Aladdin Chemical, 99%), sulfides (J&K Scientific Ltd. and Energy Chemical, >97%). All chemical reagents and solvents used were purchased from commercial sources without further purification.

The FT-IR spectra were collected in the range of 4000-400 $cm^{-1}$ on a Nicolet 170SXFT/IR spectrometer with KBr pellets dispersed samples. The powder X-ray diffraction (PXRD) pattern on the samples were recorded on a Rigaku D/max-2550 diffractometer with Cu-$K_\alpha$ radiation ($\lambda$ = 0.154 nm; scan speed = 5° $min^{-1}$; 2$\theta$ = 5–50°) at room temperature. Thermogravimetric (TGA) data were collected on a Shimadzu DTG-60AH thermal analyzer under $N_2$ atmosphere with a heating rate of 10 °C $min^{-1}$. X-ray photoelectron spectroscopy (XPS) (Escalab Xi+, Thermo Fisher Scientific Pvt. Ltd., UK) photoelectron spectrometer with a monochromatized Al-Kα X-ray source. The Elemental analyses (C, H, and N) were performed on a Perkin Elmer 240C elemental analyzer. The starting materials were commercially available and were used without further purification. After the catalytic reaction, the oxidation of sulfides was performed on a gas chromatograph (Shimadzu GC-2014C) with a flame ionization detector (FID) and equipped with a HP-5 ms capillary column. $^1$H NMR and $^{13}$C NMR spectra of the organic compounds were acquired on a AVANCE NEO 500 spectrometer by using $CDCl_3$ as the solvent and TMS (tetramethylsilane) as the internal reference. Electron paramagnetic resonance (EPR) spectra was measured by EPR-200Plus.

## X-ray crystallography

All crystallographic data were recorded at 298 K on a Bruker APEX-II CCD detector with graphite monochromatic Mo-Kα radiation ($\lambda$ = 0.71073 Å). The structures were solved by the direct methods and refined by full-matrix least-squares refinements based on $F^2$ using the SHELXTL crystallographic software package.[1,2] All the non-hydrogen atoms were refined anisotropically. The positions of hydrogen atoms on carbon atoms were calculated theoretically. Parameters of the crystal data collection and refinement are given in Table S1. The Cambridge

Crystallographic Data Centre (CCDC) number is 2164341, 1918839.

## Synthesis of $\{[Zn(1\text{-}pIM)_3]_2[Zn_6(AsW_9O_{33})_2(1\text{-}pIM)_6]\cdot 2(1\text{-}HpIM)\cdot 2H_2O\}_n$ (LCU-20)

$Na_2WO_4\cdot 2H_2O$ (0.04 g, 0.12 mmol) and $NaAsO_2$ (0.02 g, 0.12 mmol) were dissolved in 5 mL $H_2O$, $ZnCl_2$ (0.02 g, 0.15 mmol) and 1-pIM (0.14 mL, 1.23 mmol) were dissolved in 5 mL $H_2O$, Then the solution was added dropwise to the above mixture. The resulting mixture was adjusted to pH = 6.0 with 4 mol / L HCl. The solution was then sealed in a 15 mL teflon reactor and heated at 120 °C for 3 days. White crystals suitable for X-ray diffraction were obtained. Yield: 53.5%. Elemental analyses found (calcd) for $C_{84}H_{146}As_2N_{28}O_{68}W_{18}Zn_8$ ($M$ = 6618.38): C, 15.23 (15.25); H, 2.21 (2.19); N, 5.92 (5.91); As, 2.26 (2.29); W, 49.99 (49.94); Zn, 7.91 (7.88). IR (KBr, $cm^{-1}$): 3439 (s, H2O), 3131 (s, N-H), 2982 (m), 1624 (v), 1534 (v), 1464 (m), 1351 (v), 1252 (v), 1112 (s), 1012 (s), 969 (s), 921(s), 863 (s, As-O), 797 (s, W-O), 663 (m, Zn-O), 532 (s).

## Synthesis of $\{[Zn(1\text{-}ipIM)_3]_2[Zn_6(SbW_9O_{33})_2(1\text{-}ipIM)_6]\cdot 2(1\text{-}HipIM)\}_n$ (LCU-21)

Solid samples of $Na_2WO_4\cdot 2H_2O$ (0.04 g, 0.12 mmol) and $Sb_2O_3$ (0.035 g, 0.12 mmol) were dissolved in 5 mL $H_2O$, $ZnCl_2$ (0.02 g, 0.15 mmol) and 1-ipIM (0.14 mL, 1.23 mmol) were dissolved in 5 mL $H_2O$, Then the solution was added dropwise to the above mixture. The resulting mixture was adjusted to pH = 6.5 with 4 mol / L HCl. The solution was then sealed in a 15 mL teflon reactor and heated at 160 °C for 3 days. White crystals suitable for X-ray diffraction were obtained. Yield: 50.6%. Elemental analyses found (calcd) for $C_{84}H_{142}N_{28}O_{66}Sb_2W_{18}Zn_8$ ($M$ = 6676.01): C, 15.11 (15.18); H, 2.14 (2.19); N, 5.88 (5.91); Sb, 3.65 (3.69); W, 49.57 (49.54); Zn, 7.84 (7.81). IR (KBr, $cm^{-1}$): 3391 (s), 3130 (s), 3062 (w), 2956 (w), 2867 (w), 1901 (w), 1713 (w), 1636 (w), 1579 (w), 1520 (w), 1462 (w), 1374 (w), 1300 (w), 1243 (w), 1102 (s), 948 (s), 834 (s), 726 (s), 485 (s).

## Typical procedure of the oxidation reaction of sulfides catalyzed by LCU-20

In a quartz glass tube (with 22 mm of external diameter, 2 mm of wall thickness, 110 mm of height), aromatic sulfides (0.5 mmol), **LCU-20** (0.06 mol %) and methanol (2 mL) was then added and the mixture was magnetically stirred and irradiated by visible-light irradiation (10 W white LEDs, λ = 650 ± 10 nm, 10 W × 10, Xi 'an Wattecs Experimental Equipment Co., LTD., China) and simultaneously stirred at 500 rpm at room temperature under a molecular oxygen

atmosphere (1 atm., balloon) in a Wattecs Parallel Photocatalytic Reactor (WP-TEC-1020HSL) for appropriate reaction time (monitored by GC). After reaction completion as checked by GC/MS and NMR, the catalyst was separated by centrifugation and washed with methanol.

**Table S1** Crystallographic data for **LCU-20** and **-21**.

| | **LCU-20** | **LCU-21** |
|---|---|---|
| Empirical formula | $C_{84}H_{146}As_2N_{28}O_{68}W_{18}Zn_8$ | $C_{84}H_{142}N_{28}O_{66}Sb_2W_{18}Zn_8$ |
| Fw | 6618.38 | 6676.01 |
| *T*/K | 298.15 | 298.15 |
| Crystal system | monoclinic | tetragonal |
| Space group | $P2_1/n$ | $P4_2/n$ |
| *a*/ Å | 14.8816(12) | 31.704(3) |
| *b*/ Å | 24.477(2) | 31.704(3) |
| *c*/ Å | 20.8035(19) | 14.8740(13) |
| $\alpha$ (°) | 90 | 90 |
| $\beta$ (°) | 93.075(10) | 90 |
| $\gamma$ (°) | 90 | 90 |
| *V* / Å$^3$ | 7566.9(11) | 14951(3) |
| *F* (000) | 6056.0 | 12176.0 |
| *Z* | 2 | 4 |
| $\rho_{calcd}$ (g·cm$^{-3}$) | 2.905 | 2.966 |
| $\mu$ (mm$^{-1}$) | 15.381 | 15.482 |
| $R_1[I>2\sigma(I)]$ | 0.0674 | 0.0547 |
| $wR_{2b}[I>2\sigma(I)]$ | 0.1648 | 0.1117 |
| $R_1$(all data) | 0.1125 | 0.1038 |
| $wR_{2b}$ (all data) | 0.1909 | 0.1259 |
| GOOF of F$^2$ | 1.070 | 0.942 |
| CCDC No. | 2164341 | 1918839 |

$R_1 = \sum||F_o|-|F_c||/\sum|F_o|$. $wR_2 = \{\sum[w(F_o^2-F_c^2)^2]/\sum[w(F_o^2)^2]\}^{1/2}$

**Table S2** Selected bond lengths [Å] and angles [º] for **LCU-20** and **-21**.

| | | | |
|---|---|---|---|
| **LCU-20** | | | |
| W1-O1 | 2.379(14) | W1-O4 | 1.694(14) |
| W1-O4 | 1.694(14) | Zn1-N1 | 2.03(2) |
| As1-O1 | 1.802(13) | N1-C1 | 1.30(3) |
| Zn1-O16 | 2.094(13) | C8-C9 | 1.35(4) |
| O4-W1-O1 | 170.4(6) | N1-Zn1-O16 | 116.8(8) |
| O2-As1-O1 | 96.5(6) | As1-O1-W1 | 135.0(7) |
| O16-Zn1-O9 | 146.7(5) | W7-O26-Zn3 | 133.5(7) |
| Zn3-O24-Zn1 | 99.2(6) | C3-C2-N1 | 108(3) |
| **LCU-21** | | | |
| W1-O3 | 2.248(11) | W1-O4 | 1.987(11) |
| Sb1-O1 | 1.981(11) | Zn2-O13 | 2.075(11) |
| Zn1-O11 | 2.058(11) | N3-C7 | 1.28(3) |
| Zn1-N1 | 2.00(2) | C2-C3 | 1.32(4) |
| O4-W1-O3 | 73.8(4) | N1-Zn1-O11 | 99.4(8) |
| O1-Sb1-O2 | 90.4(5) | W1-O5-Zn4 | 168.3(7) |
| O11-Zn1-O13 | 90.8(5) | Zn1-O13-Zn2 | 99.2(5) |
| N1-Zn1-O13 | 106.6(8) | Sb1-O3-W1 | 115.4(5) |

**Table S3** Optimization of the reaction conditions for photooxidation of MPS[a].

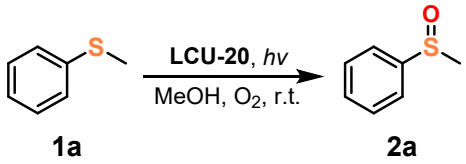


| Entry | Photosources | Catalysts | Yield (%)[b] | Sele. (%)[c] |
|---|---|---|---|---|
| 1 | White | **LCU-20** | 99 | 99 |
| 2[d] | White | **LCU-20** | -- | -- |
| 3 | White | $Na_2WO_4$ | trace | trace |
| 4 | White | $ZnCl_2$ and $Na_2WO_4$ | 10 | 99 |
| 5[e] | White | **LCU-20** | -- | -- |
| 6[f] | White | **LCU-20** | -- | -- |

[a]Reaction conditions: MPS (0.5 mmol), $O_2$ (1 atm), **LCU-20** (0.06 mol%), and 2 mL methanol, chlorobenzene as an internal standard, white LED light (10 W) for 36 hours. [b]Yields were determined by GC using an internal standard technique. [c]The by-products were the corresponding sulfones. [d]The reaction was conducted without oxidant ($O_2$). [e]Adding $NaN_3$ as radical quencher. [f]Adding 2,2,6,6-tetramethyl-1-piperidinyloxy (TEMPO) as electrons trapper.

**Table S4** The influence of different LEDs on the photooxidation of MPS[a].

| Entry | LED | λp (nm) | Yield (%)[b] | Sele. (%)[c] |
|---|---|---|---|---|
| 1 | Blue | 460 ± 10 | 68 | 71 |
| 2 | Green | 520 ± 10 | 76 | 78 |
| 3 | Orange | 590 ± 10 | 80 | 82 |
| 4 | Red | 630 ± 10 | 89 | 91 |
| 5 | White | Continous | 99 | 99 |

[a]Reaction conditions: MPS (0.5 mmol), $O_2$ (1 atm), **LCU-20** (0.06 mol%), LEDs (λp =λ ± 10 nm, 10 W × 10) and 2 mL methanol, chlorobenzene as an internal standard for 36 hours. [b]Yields were determined by GC using an internal standard technique and were based on sulfides. [c]The byproducts were the corresponding sulfones.

**Table S5** The results of the oxidation of sulfides catalyzed by various POMs photocatalyst.

| Catalysts | Reaction conditions | Results | Ref. |
|---|---|---|---|
| **LCU-20** | 10 W White light, $O_2$, 25°C | yield 99% | This work |
| $((n\text{-}C_4H_9)_4N)_5[SiW_{11}(Sn(CH_2)_2HCNC_{16}H_9)O_{39}]$ | 150W Xe lamp, $O_2$, 25°C | yield 87% | [3] |
| $TBA_4H[\gamma\text{-}PV_2W_{10}O_{40}]$ | Xe lamp, $\lambda > 400$ nm, $O_2$, 30°C | yield 92% | [4] |
| $(C_2H_8N)_6[SiW_{11}CdO_{39}][Ru(bpy)_2(dcbpy)]\cdot DMF\cdot 5.5H_2O$ | 10 W White light, $O_2$, 25°C | yield 99.5% | [5] |
| $TPPV_{10}$ (TPP = tetraphenylphosphonium) | Xe lamp, $\lambda$ >400nm, $O_2$, 30°C | yield 93% | [6] |
| $Co(Mo_4O_{13})(TPT)_2$ (TPT = 2,4,6-tri(4-pyridyl)-1,3,5-triazine) | 10 W White light, $O_2$, 30°C | yield 96.3% | [7] |

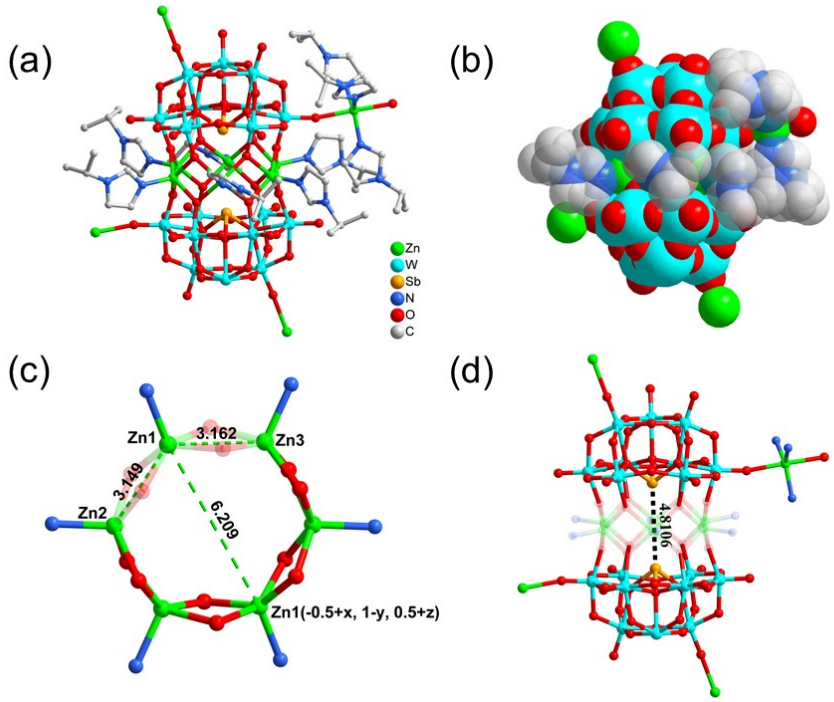


**Fig. S1** (a) Ball-and-stick view of **LCU-21**. (b) Space-filling structure of the **LCU-21**. (c) The six nuclear Zn cluster in **LCU-21**. (d) The distance between heteroatoms (Sb❿❿❿Sb) in the **LCU-21**. H atoms and lattice solvent molecules are omitted for clarity. Color codes: Zn, green; W, turquiose; As, yellow; Sb, light orange; N, light blue; O, red; C, gray.

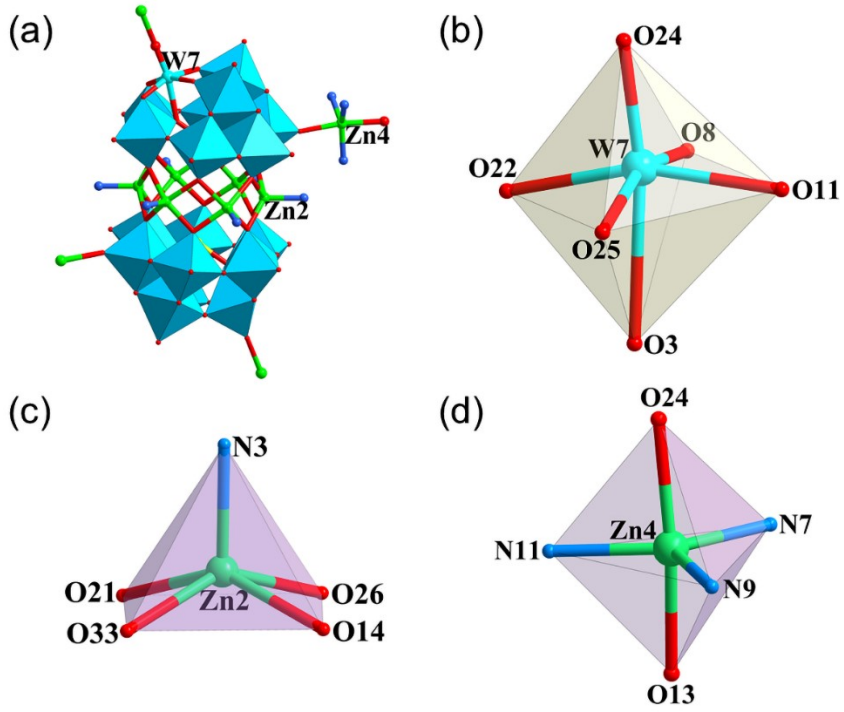


**Fig. S2** (a) Polyhedral and ball-and-stick of **LCU-20**. (b) The coordination environment of W7. (c) The coordination environment of Zn2. (d) The coordination environment of Zn4.

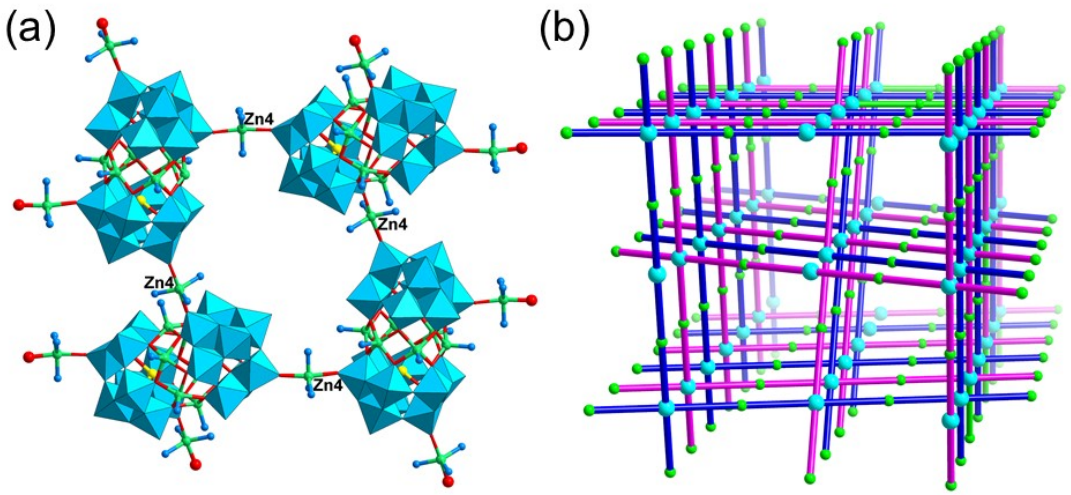


**Fig. S3** (a) The connection of polyanions to the neighbor clusters with Zn centers (Zn4) in **LCU-21**. (b) Schematic presentations of the 2-fold interpenetrated 4-connected *lvt* networks of **LCU-21**.

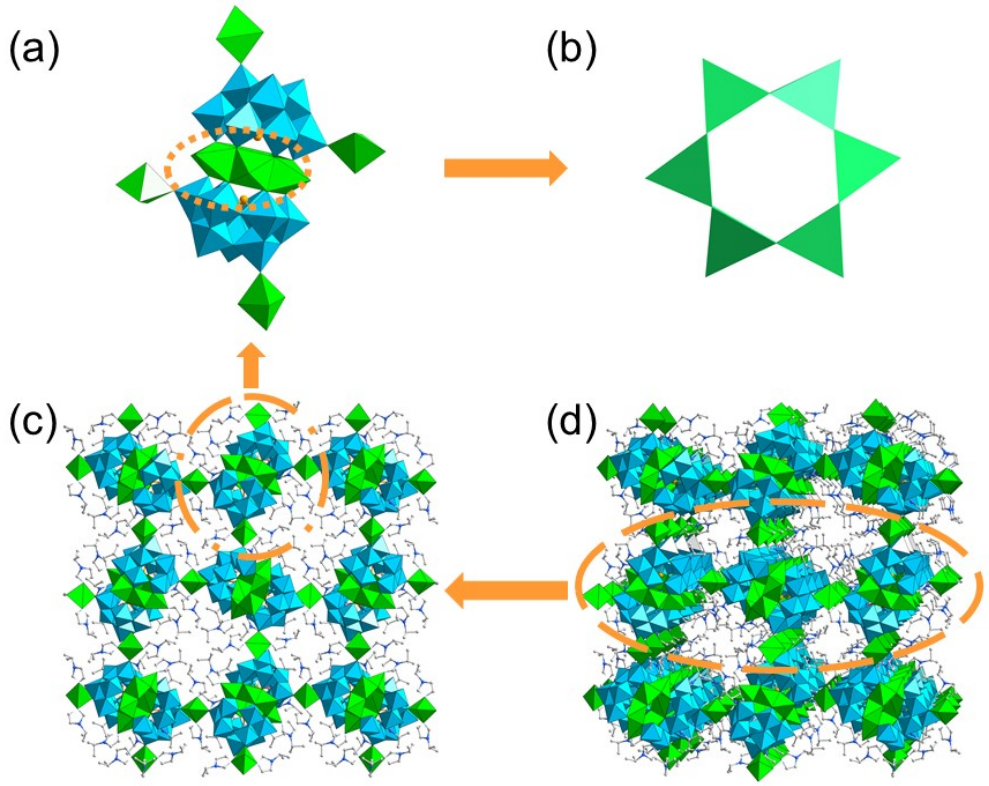


**Fig. S4** (a) Polyhedral view of the **LCU-21**. (b) Polyhedral view of the $Zn_6$ hexagonal ring in **LCU-21**. (c) 2D layer structure of **LCU-21**. (d) 3D packing structure of **LCU-21**.

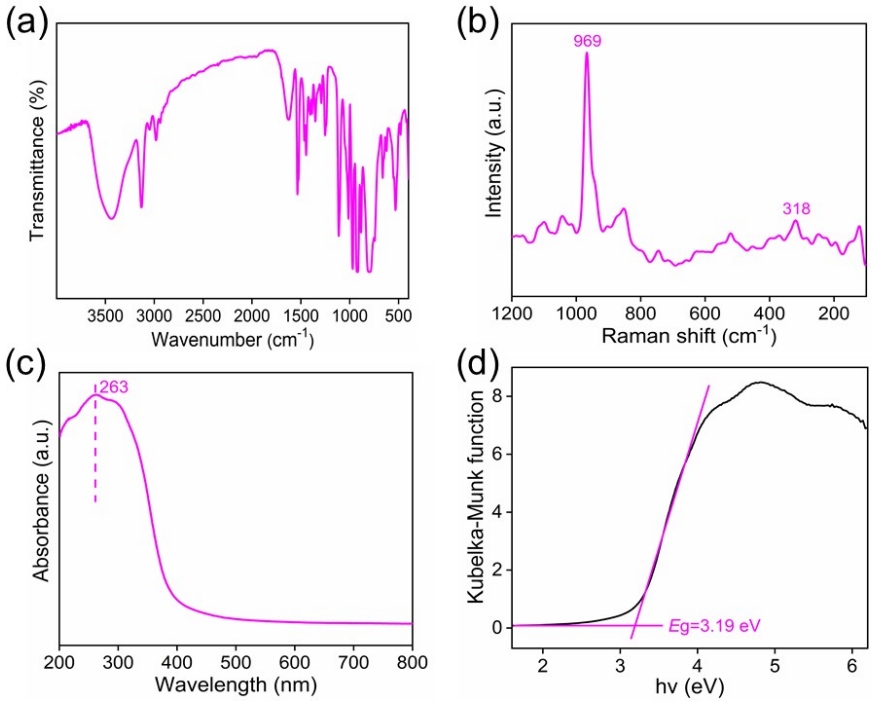


**Fig. S5** (a) FT-IR spectrum of **LCU-20**. (b) Raman spectrum of **LCU-20**. (c) solid-state UV-Vis DRS (absorbance vs. wavelength) of **LCU-20**. (d) Solid-state UV–Vis DRS (Kubelka-Munk Function vs. Energy) of **LCU-20**.

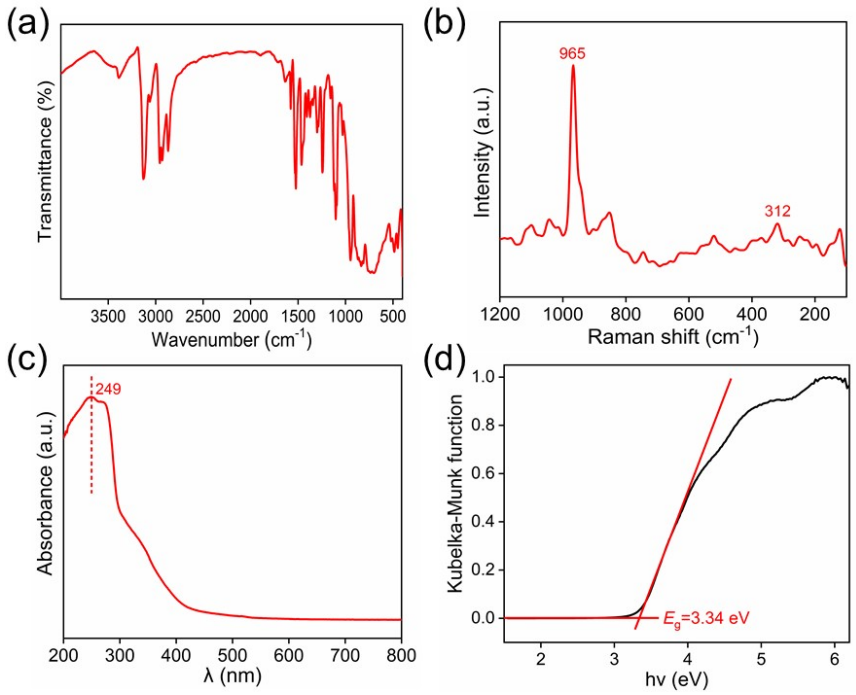


**Fig. S6** (a) FT-IR spectrum of **LCU-21**. (b) Raman spectrum of **LCU-21**. (c) Solid-state UV-Vis DRS (absorbance vs. wavelength) of **LCU-21**. (d) Solid-state UV–Vis DRS (Kubelka-Munk Function vs. Energy) of **LCU-21**.

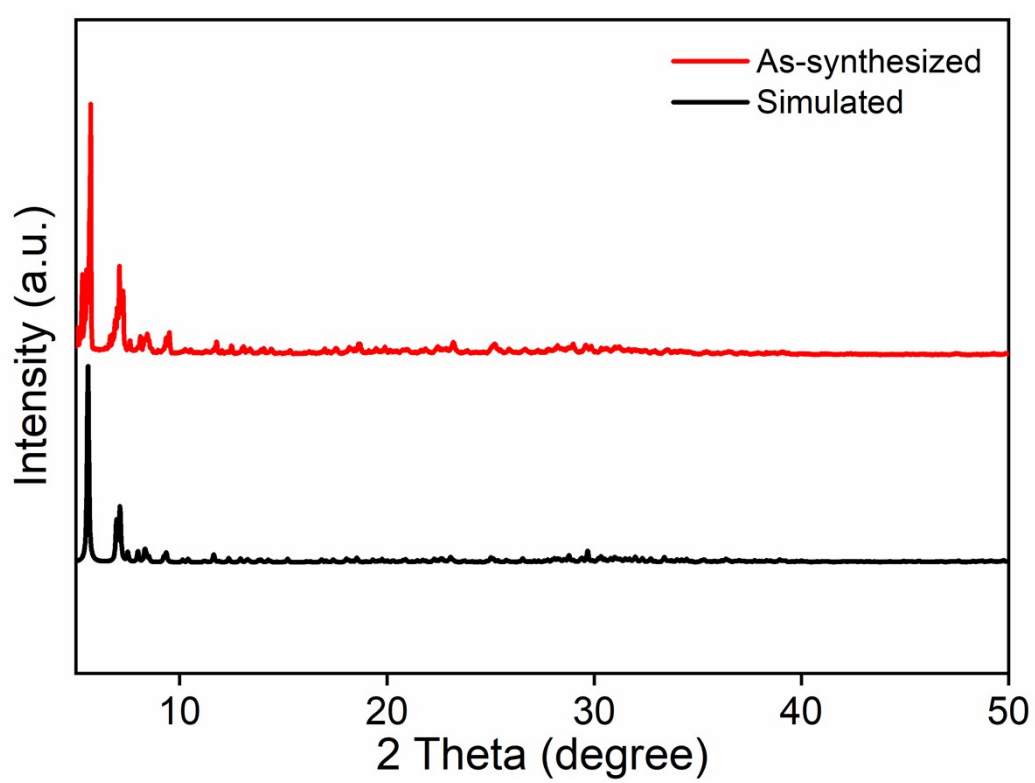


**Fig. S7** The simulated and experimental PXRD patterns of **LCU-20**.

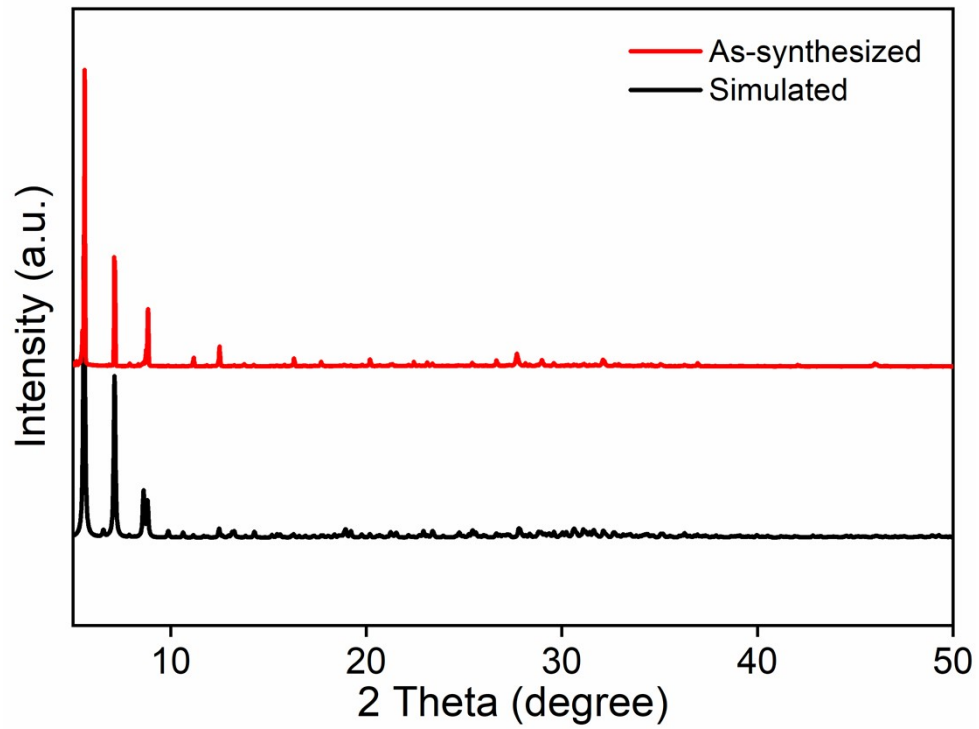


**Fig. S8** The simulated and experimental PXRD patterns of **LCU-21**.

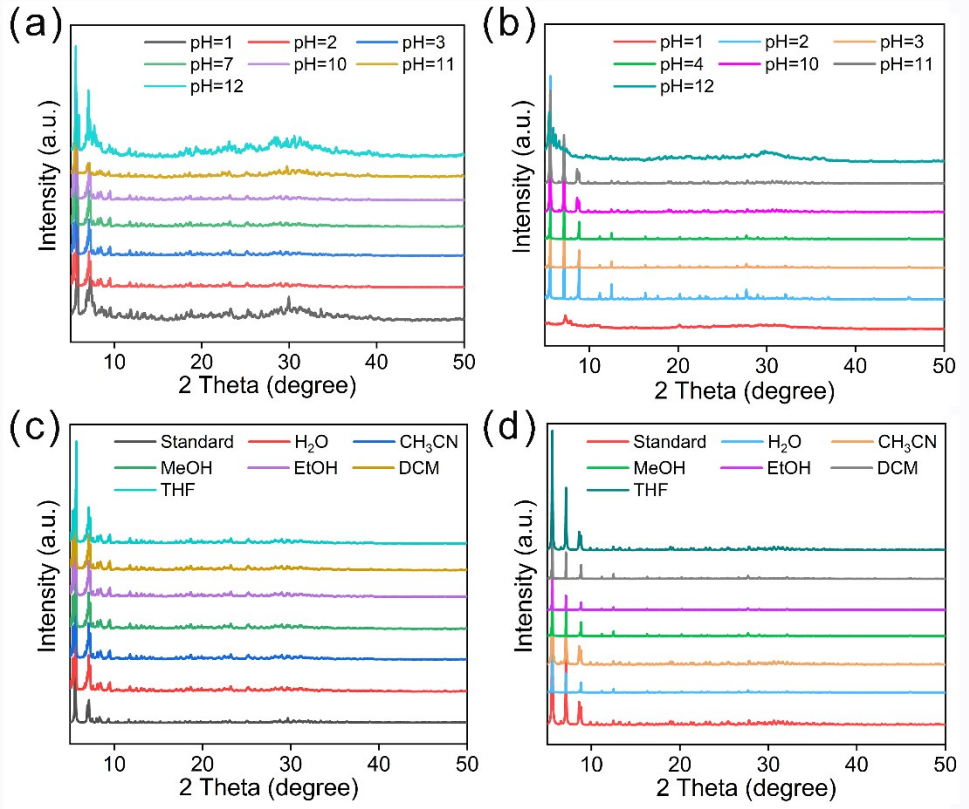


**Fig. S9** PXRD patterns of **LCU-20** and **-21** after immersed in different solutions at room temperature for 24 hours. (a) Various pH values for **LCU-20**. (b) Various pH values for **LCU-21**. (c) Various solvents for **LCU-20**. (d) Various solvents for **LCU-21**.

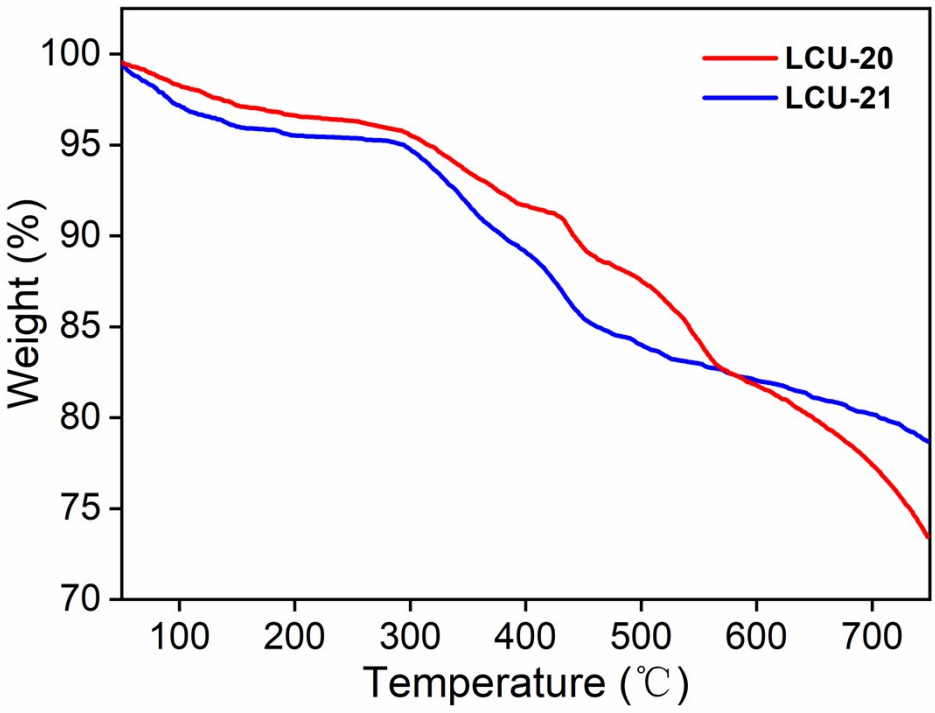


**Fig. S10** TGA curves of **LCU-20** and **-21**.

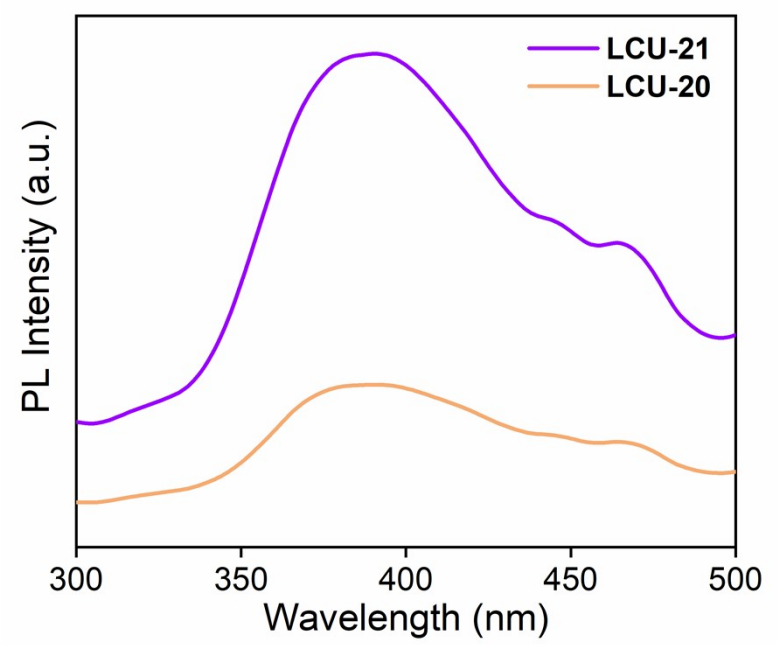


**Fig. S11** Photoluminescence spectra of **LCU-20** and **LCU-21**

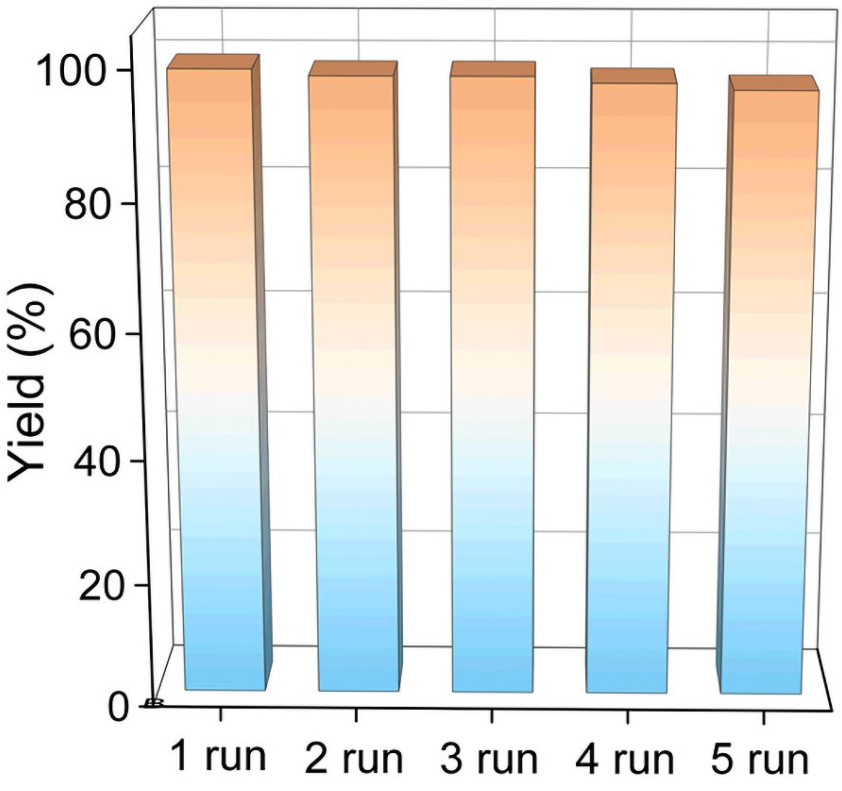


**Fig. S12** The results of photooxidation of MPS by **LCU-20** in five reused experiments.

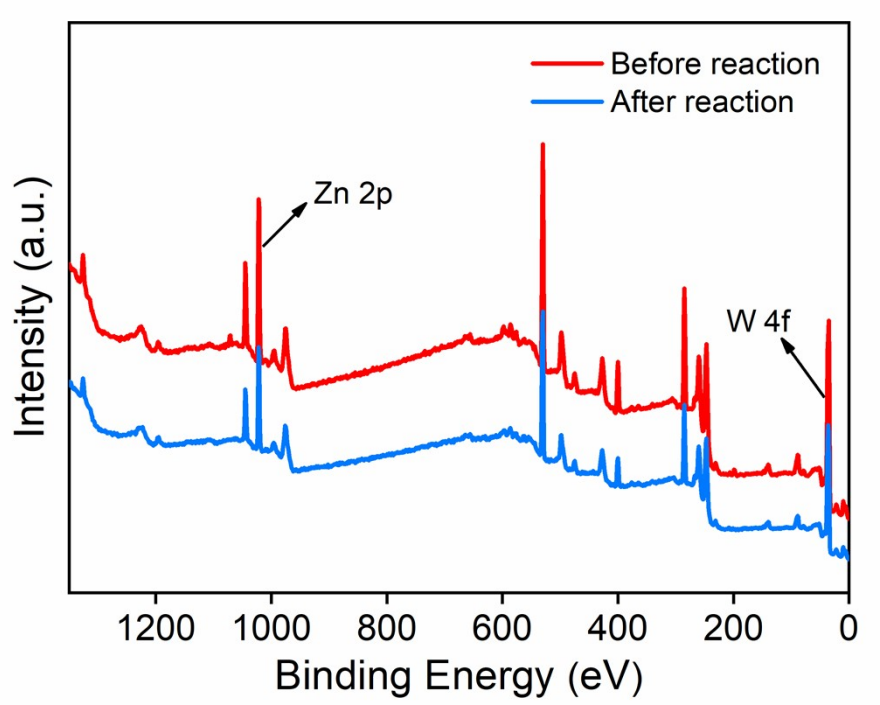


**Fig. S13** XPS spectra of **LCU-20** before and after five runs reactions.

## Leaching test for the photooxidation of MPS by LCU-20.

Regarding the leaching experiment, all the details were the same with the typical procedure for photocatalytic test mentioned in this paper, the reaction was stopped and the photocatalyst was removed by centrifugal filtration. After removing the catalyst, the filtrate was restarted under the optimal conditions. The yields of MPSO were detected at intervals throughout the reaction time.

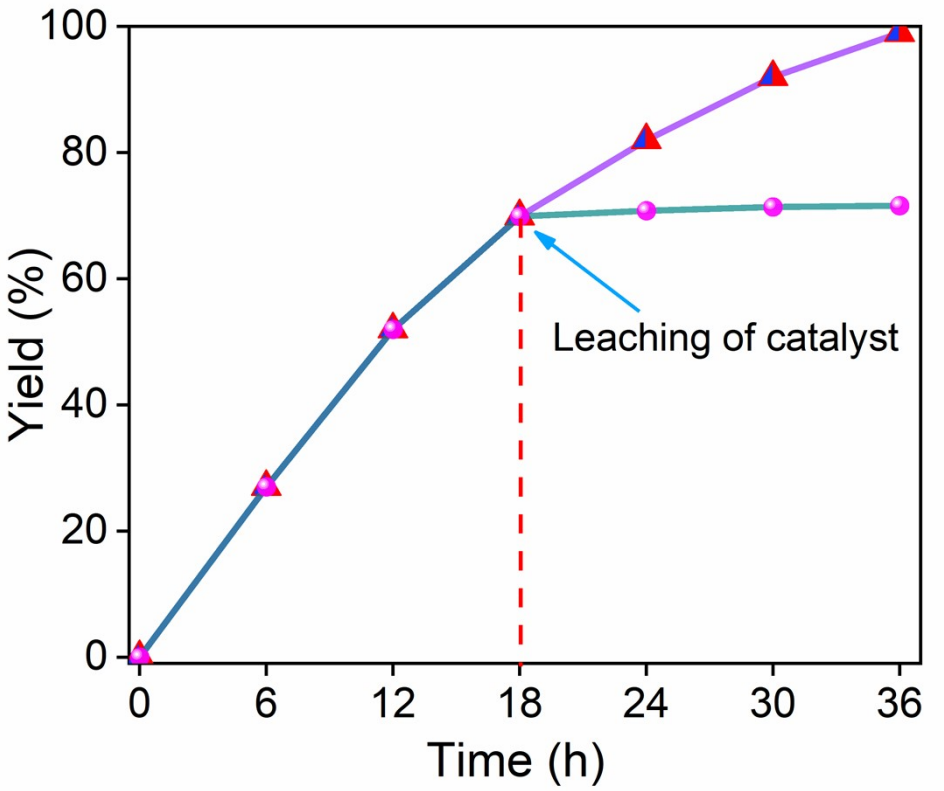


**Fig. S14** Leaching test for the photooxidation of MPS by **LCU-20**.

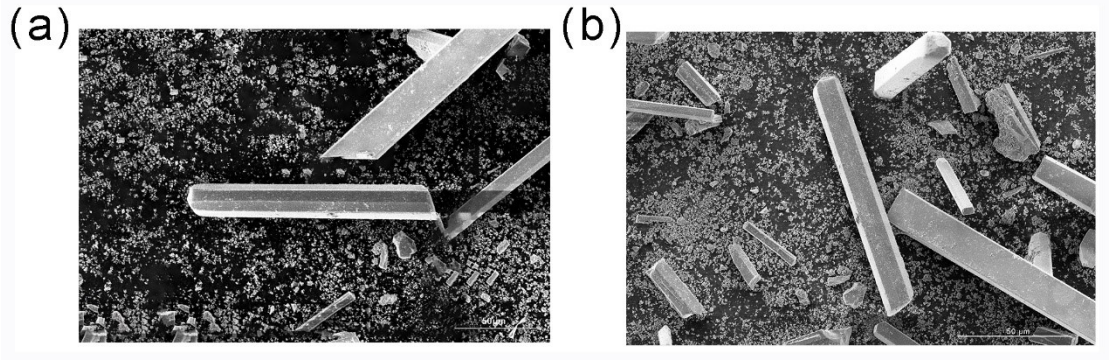


**Fig. S15** SEM images of **LCU-20** (a) before and (b) after five runs reactions.

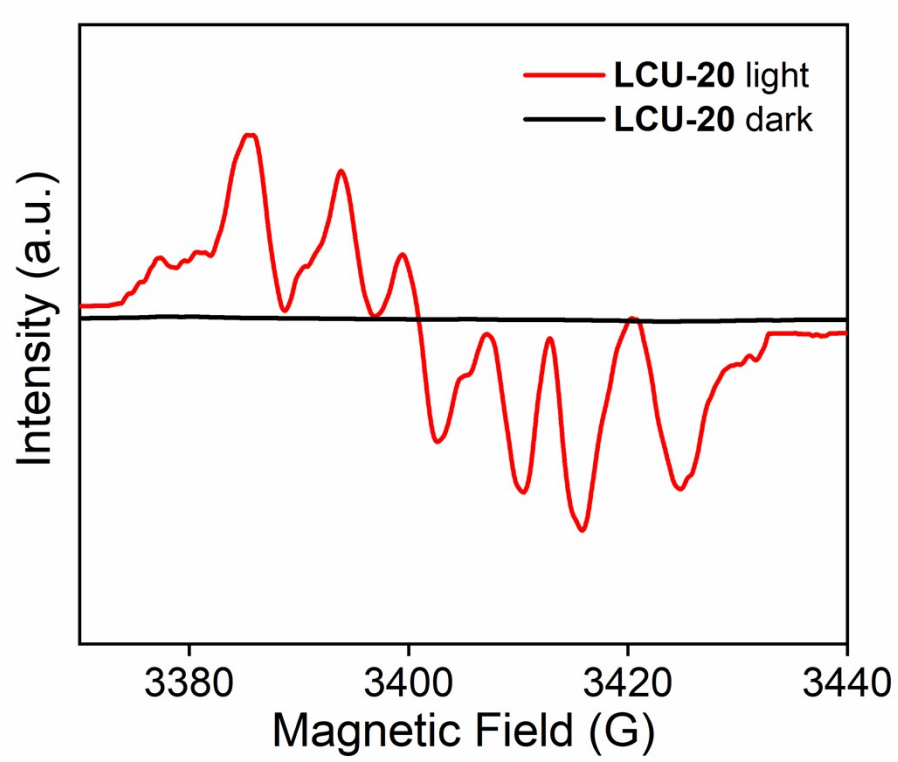


**Fig. S16** EPR spectra for detecting of superoxide radical: spin trapping of $O_2^{\bullet-}$ with 5,5-dimethyl-1-pyrroline N-oxide (DMPO).

**Fig. S17** The picture of photocatalytic reactor.

## NMR data of sulfoxides

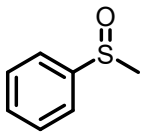

**2a**: $^{1}$H NMR (500 MHz, $CDCl_3$) δ 7.63 (dd, *J* = 8.0, 1.6 Hz, 2H), 7.53 – 7.45 (m, 3H), 2.70 (s, 3H); $^{13}$C NMR (126 MHz, $CDCl_3$) δ 131.10, 129.42, 127.39, 123.54, 44.01.

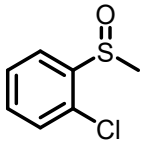

**2b**: $^{1}$H NMR (500 MHz, $CDCl_3$) δ 7.91 (dd, *J* = 7.8, 1.6 Hz, 1H), 7.49 (td, *J* = 7.5, 1.3 Hz, 1H), 7.41 (td, *J* = 7.6, 1.7 Hz, 1H), 7.35 (dd, *J* = 7.9, 1.3 Hz, 1H), 2.78 (s, 3H); $^{13}$C NMR (126 MHz, $CDCl_3$) δ 143.53, 132.03, 129.79, 128.19, 125.29, 41.64.

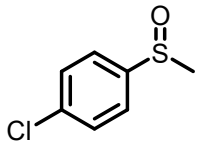

**2c**: $^{1}$H NMR (500 MHz, $CDCl_3$) δ 7.88 (d, *J* = 8.6 Hz, 2H), 7.57 – 7.52 (m, 2H), 3.05 (s, 3H); $^{13}$C NMR (126 MHz, $CDCl_3$) δ 140.57, 139.14, 129.82, 129.03, 125.08, 44.64.

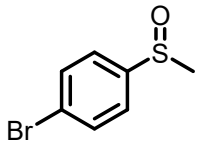

**2d**: $^{1}$H NMR (500 MHz, $CDCl_3$) δ 7.80 (d, *J* = 8.6 Hz, 2H), 7.71 (d, *J* = 8.6 Hz, 2H), 3.05 (s, 3H); $^{13}$C NMR (126 MHz, $CDCl_3$) δ 139.66, 132.83, 129.10, 44.62.

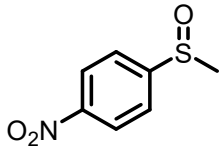

**2e**: $^{1}$H NMR (500 MHz, $CDCl_3$) δ 8.43 (d, *J* = 8.8 Hz, 2H), 8.16 (d, *J* = 8.8 Hz, 2H), 3.12 (s, 3H); $^{13}$C NMR (126 MHz, $CDCl_3$) δ 151.00, 146.08, 129.11, 124.78, 44.42.

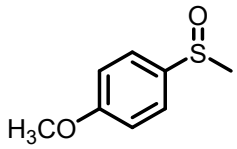

**2f**: $^{1}$H NMR (500 MHz, $CDCl_3$) δ 7.27 (d, *J* = 8.8 Hz, 2H), 6.85 (d, *J* = 8.8 Hz, 2H), 3.78 (s, 3H), 2.44 (s, 3H); $^{13}$C NMR (126 MHz, $CDCl_3$) δ 158.28, 130.27, 128.86, 114.70, 55.45, 18.16.

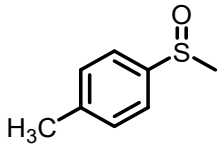

**2g**: $^{1}$H NMR (500 MHz, $CDCl_3$) δ 7.82 (d, *J* = 8.3 Hz, 2H), 7.38 – 7.34 (m, 2H), 3.03 (s, 3H), 2.45 (s, 3H); $^{13}$C NMR (126 MHz, $CDCl_3$) δ 144.79, 137.84, 130.15, 130.07, 127.49, 123.66, 44.73, 21.73.

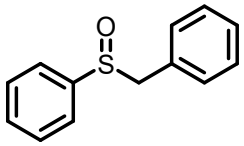

**2h**: $^{1}$H NMR (500 MHz, $CDCl_3$) δ 7.31 – 7.16 (m, 10H), 4.12 (s, 2H); $^{13}$C NMR (126 MHz, $CDCl_3$) δ 137.60, 136.50, 129.98, 128.97, 128.63, 127.32, 126.49, 39.20.

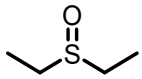

**2i**: $^{1}$H NMR (500 MHz, $CDCl_3$) δ 2.53 (q, *J* = 7.4 Hz, 4H), 1.24 (t, *J* = 7.4 Hz, 6H); $^{13}$C NMR (126 MHz, $CDCl_3$) δ 25.50, 14.83.

## GC, GC-MS and NMR spectra of sulfoxides


**Fig. S18** MS and NMR spectra of (methylsulfinyl)benzene (**2a**).

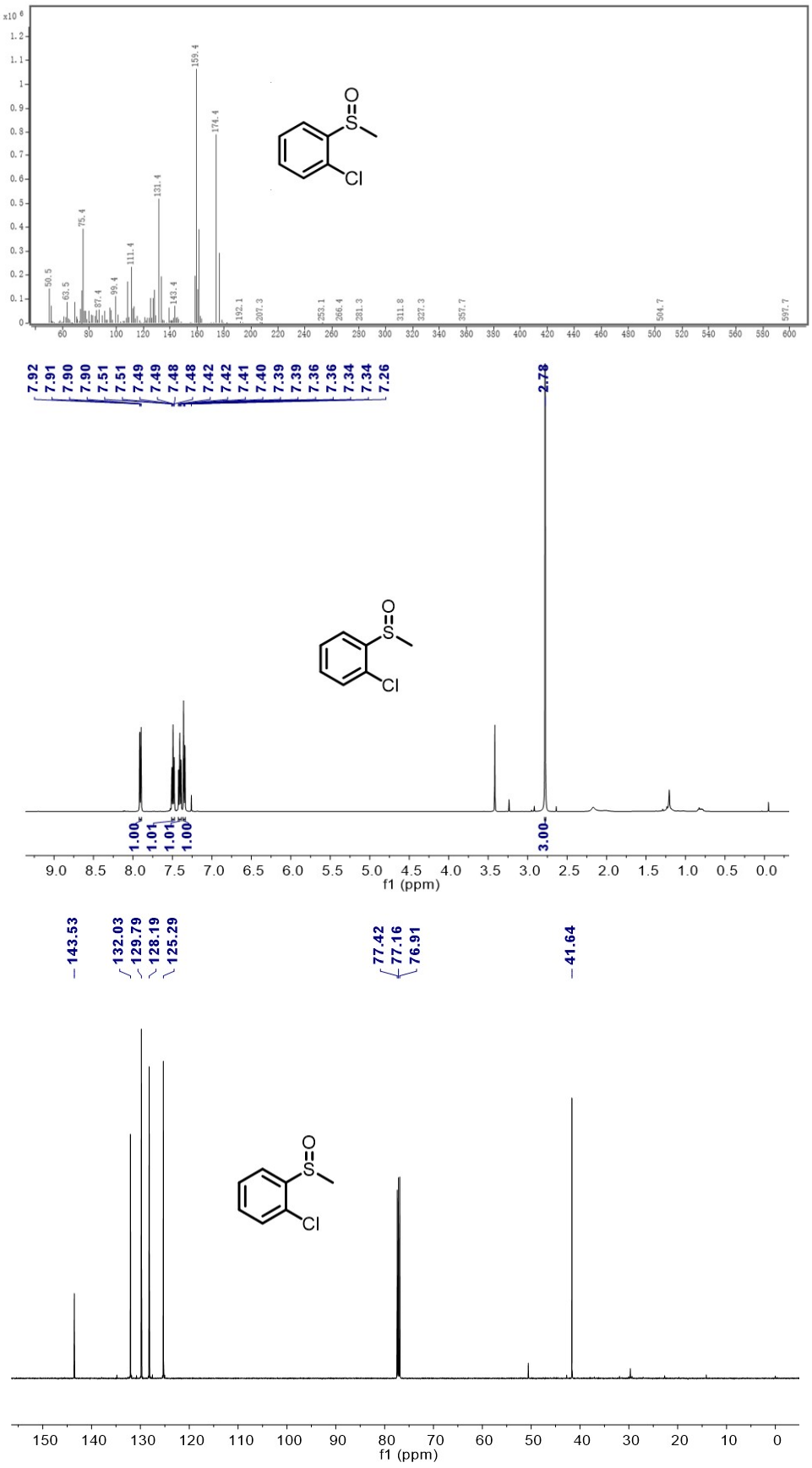


**Fig. S19** MS and NMR spectra of 1-chloro-2-(methylsulfinyl)benzene (**2b**).

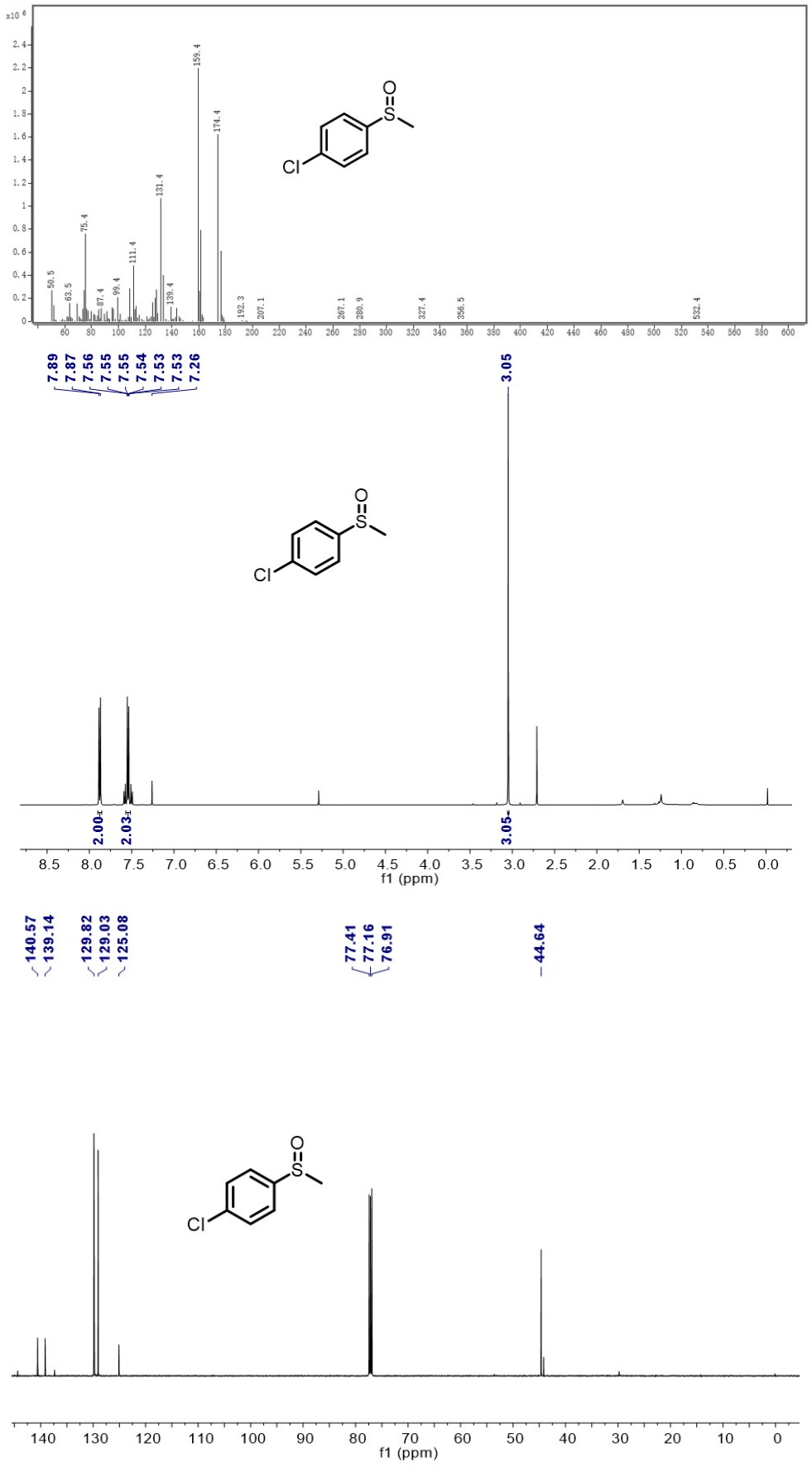


**Fig. S20** MS and NMR spectra of 1-chloro-4-(methylsulfinyl)benzene (**2c**).

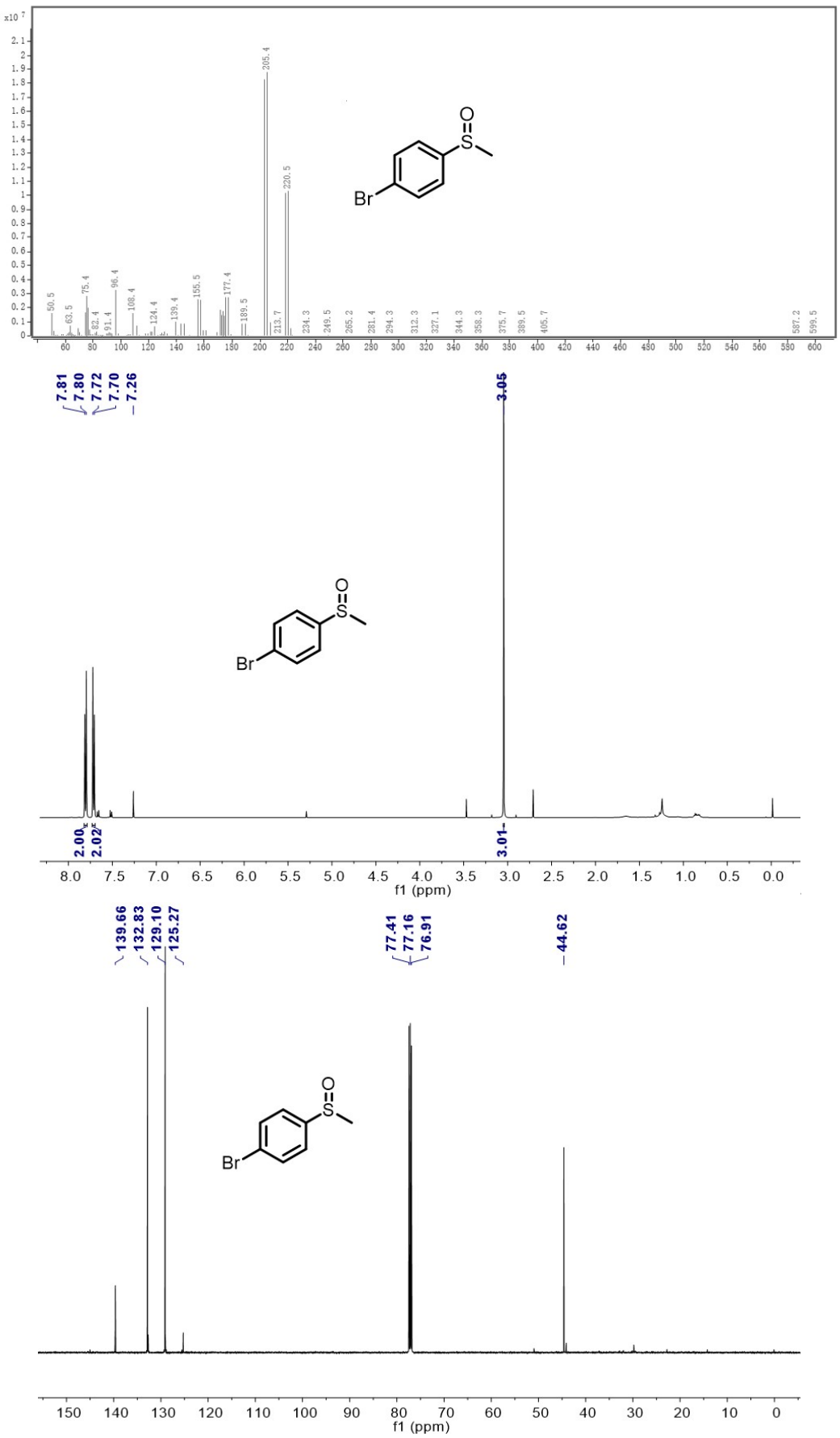


**Fig. S21** MS and NMR spectra of 1-bromo-4-(methylsulfinyl)benzene (**2d**).

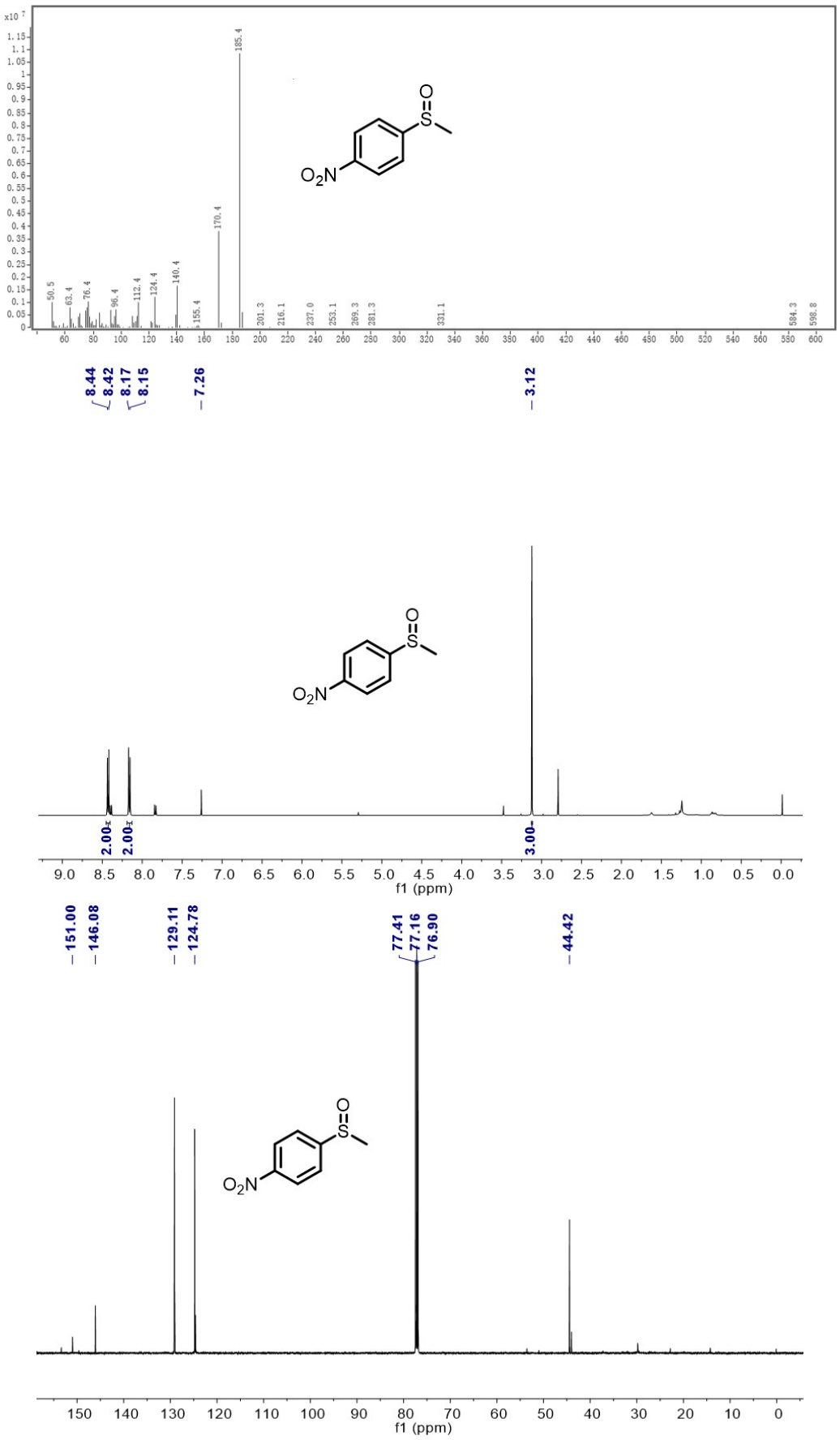


**Fig. S22** MS and NMR spectra of 1-(methylsulfinyl)-4-nitrobenzene (**2e**).

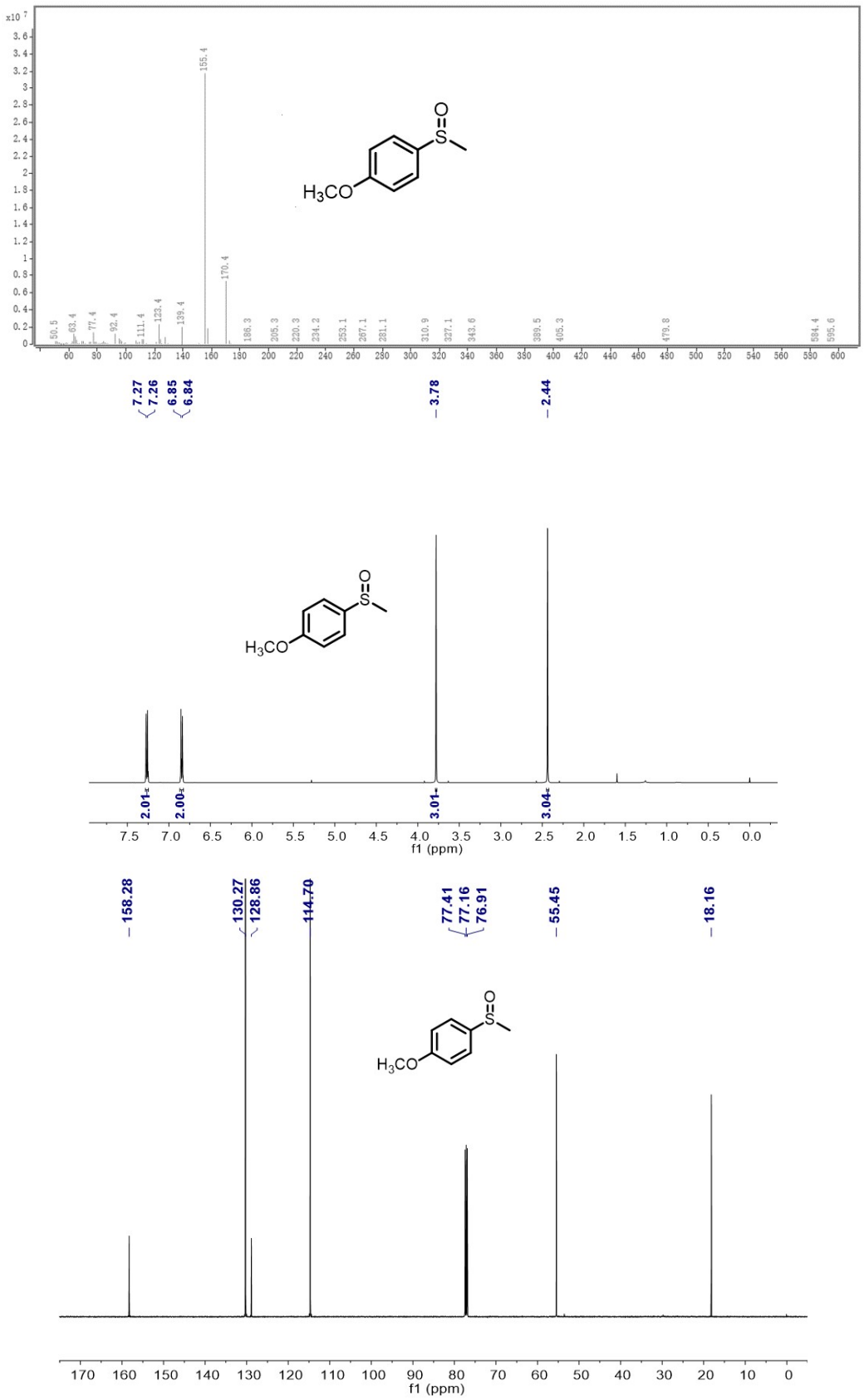


**Fig. S23** MS and NMR spectra of 1-methoxy-4-(methylsulfinyl)benzene (**2f**).

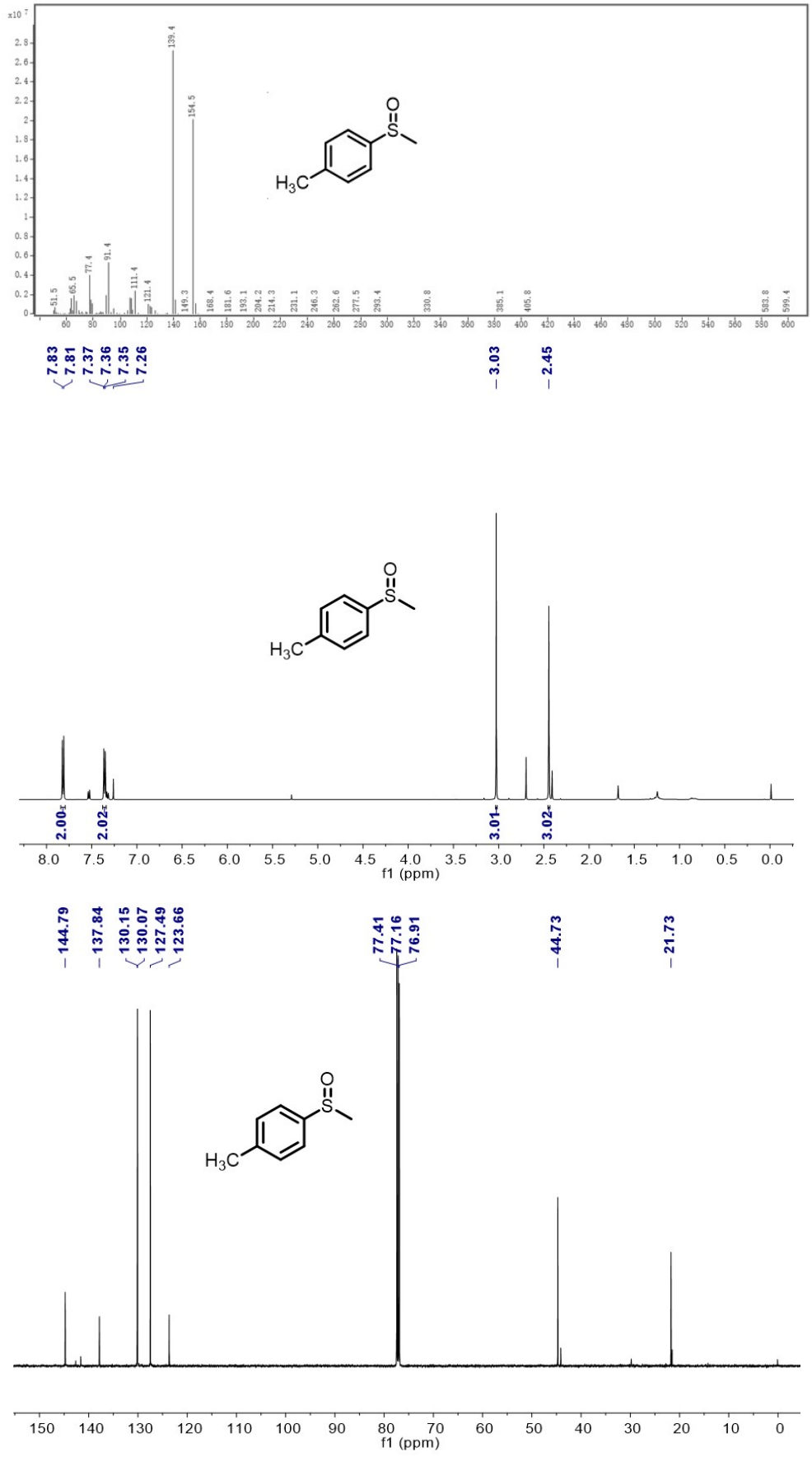


**Fig. S24** MS and NMR spectra of 1-methyl-4-(methylsulfinyl)benzene (**2g**).

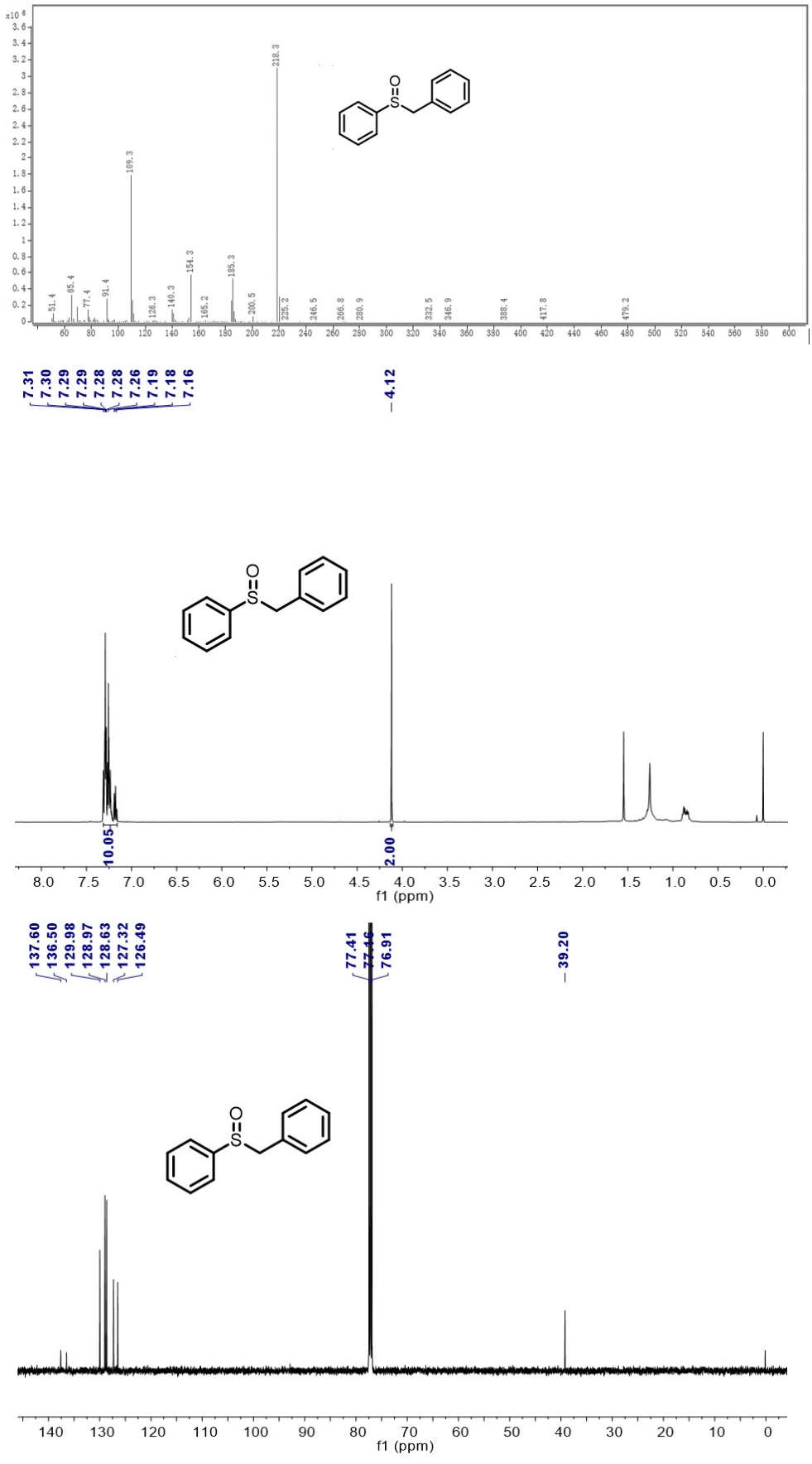


**Fig. S25** MS and NMR spectra of (benzylsulfinyl)benzene (**2h**).

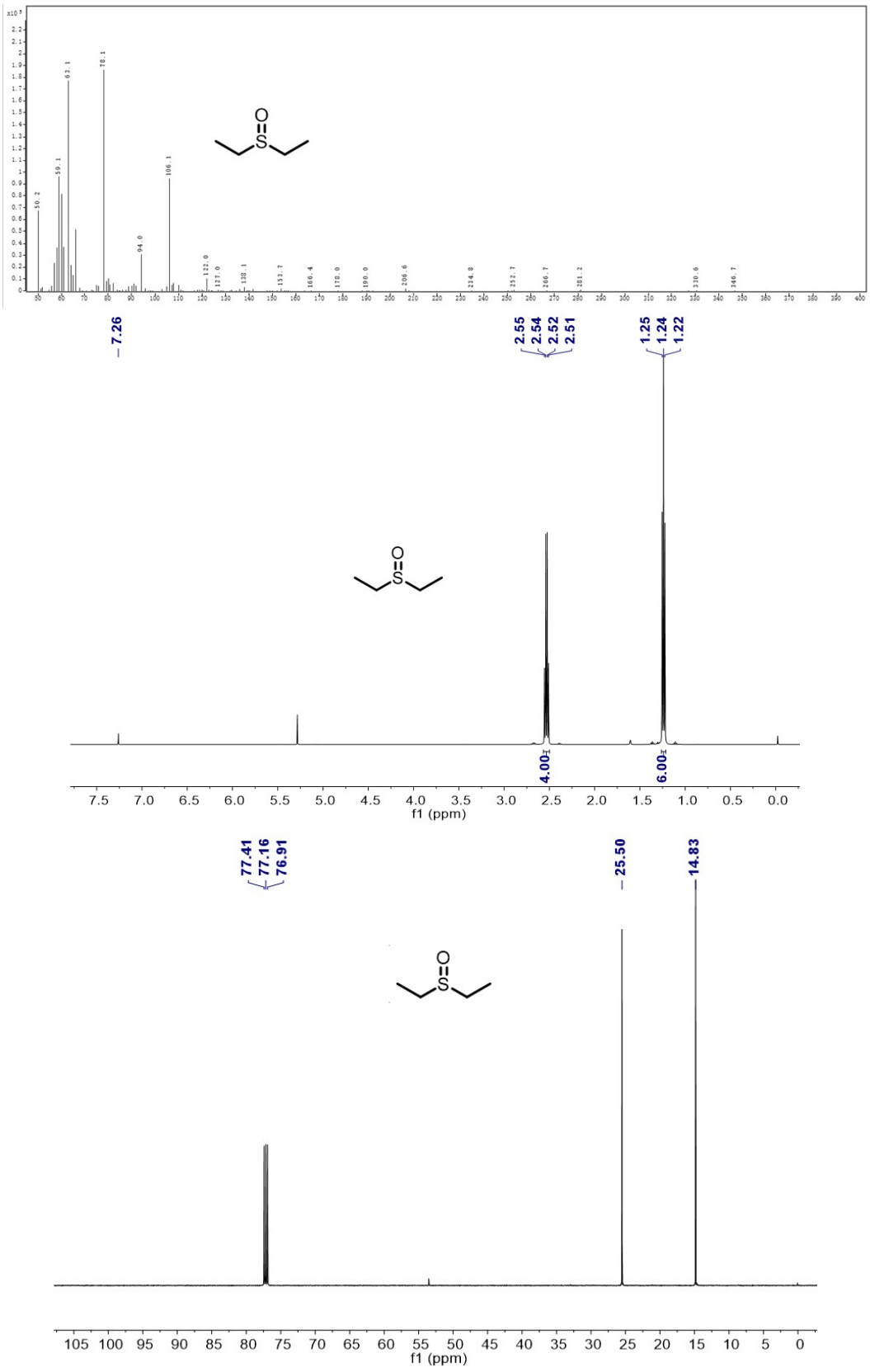


**Fig. S26** MS and NMR spectra of (ethylsulfinyl)ethane (**2i**).

## References

[1] G.M. Sheldrick, A Short History of SHELX, *Acta Cryst*., 2008, **A64**, 112–122.

[2] G. M. Sheldrick, Crystal Structure Refinement with SHELXL, *Acta Crystallogr. C: Struct. Chem*., 2015 **C71**, 3–8.

[3] D. Karimian, F. Zangi, Aerobic Photoxidation of Sulfides Using Unique Hybrid Polyoxometalate under Visible Light, *Catal. Commun.*, 2021, **152**, 106283.

[4] C. Li, K. Suzuki, N. Mizunoa, K. Yamaguchi, Polyoxometalate LUMO Engineering: a Strategy for Visible-Light-Responsive Aerobic Oxygenation Photocatalysts, *Chem. Commun.*, 2018, **54**, 7127-7130.

[5] K. Ji, Y. Liu, Y. Luo, X. Zhang, Y. Bai, H. Yue, P. Ma, J. Niu, J. Wang, Metalloligand Hybrid Polyoxometalates for Efficient Selective Photocatalytic Oxidation of Sulfides to Sulfoxides under Visible-Light Irradiation, *J. Phys. Chem. C*, 2023, **127**, 256–264.

[6] C. Li, N. Mizuno, K. Murata, K. Ishii, T. Suenobu, K. Yamaguchi, K. Suzuki, Selectivity Switch in the Aerobic Oxygenation of Sulfides Photocatalysed by Visible-Light-Responsive Decavanadate, *Green Chem*., 2020, **22**, 3896-390.

[7] X. Yan, Z. Shi, J. Jiao, C. Si, Q. Han, An Isopolymolybdate-Incorporated Metal–Organic Framework with Sulfite Oxidase-Mimicking Activity for Photocatalytic Oxidation of Sulfides Utilizing In Situ-Generated Singlet Oxygen, *Inorg. Chem.*, 2021, **60**, 16810-16816.